UDC 681.516 https://doi.org/10.20998/2074-272X.2026.1.05

H. Mostefaoui, S. Tahraoui, M. Souaihia, R. Taleb, M. Mostefaoui

Advanced control of twin rotor multi-input multi-output systems using seagull optimization for linear quadratic regulator tuning

Introduction. *During the past decade, advanced control of complex multi-input multi-output (MIMO) systems has been a sustained focus owing to their growing use in aerospace and robotic platforms. The twin rotor MIMO system (TRMS) serves as a helicopter-like benchmark system for testing advanced control techniques. Its nonlinear behavior and significant cross-coupling render it difficult to control using traditional methods.* ***Problem.*** *The TRMS features strong nonlinear dynamics and cross-coupling effects that challenge conventional control methods. Manual tuning of control parameters often results in suboptimal performance and reduced robustness. The* ***goal*** *of this study is to optimize the linear quadratic regulator (LQR) weighting matrices Q and R for the TRMS using the seagull optimization algorithm (SOA) to improve transient performance, minimize overshoot, and accelerate stabilization in both pitch and yaw compared to classical LQR tuning.* ***Methodology****. The new approach integrates the SOA with LQR control theory. The SOA determines the best values of Q and R matrices by minimizing a cost function defined by system performance metrics. SOA-optimized LQR is evaluated through simulations and contrasted with the classical LQR under identical conditions. Population size is 50 agents with a maximum of 100 iterations to achieve convergence.* ***Results.*** *Simulation results show that the SOA-optimized LQR has a remarkable improvement in the system's time response. In comparison to the classical LQR, these results provide a shorter settling time from 7.35 s to 5.34 s (≈28 %), decreases overshoot (≈3 % vs. 30 % open loop), increases damping, and reduces oscillations. The pitch and yaw angle responses across several control schemes clearly demonstrate the superior performance of the proposed optimization technique.* ***Scientific novelty****. This work demonstrates, for the first time, the use of SOA for optimal tuning of LQR in a TRMS benchmark. It opens new avenues to enhance the performance of high-order nonlinear systems, pointing toward more accurate and stable control techniques in industrial and aerospace engineering fields.* ***Practical value****. The technique provides an efficient method to enhance the functionality of complex nonlinear systems without requiring manual tuning, and it has potential applications in the industrial and aerospace areas.* References 38, tables 3, figures 4.

Key words: **seagull optimization algorithm, linear quadratic regulator, twin rotor multi-input multi-output system, parameter tuning, control performance.**

Вступ*. Протягом останнього десятиліття розширене управління складними багатовходовими та багатовихідними (MIMO) системами знаходилося в центрі уваги у зв'язку з їх зростаючим використанням в аерокосмічній техніці та робототехніці. Двороторна MIMO система (TRMS) служить еталонною системою, подібною до вертольоту, для тестування передових методів управління. Її нелінійна поведінка та значний перехресний зв'язок ускладнюють управління традиційними методами.* ***Проблема****. TRMS характеризується сильною нелінійною динамікою та ефектами перехресного зв'язку, що кидають виклик традиційним методам управління. Ручне налаштування параметрів керування часто призводить до неоптимальних характеристик та зниження надійності.* ***Метою*** *роботи є оптимізація вагових матриць Q і R лінійно-квадратичного регулятора (LQR) для TRMS з використанням алгоритму оптимізації «чайка» (SOA) для покращення перехідних характеристик, мінімізації перерегулювання та прискорення стабілізації як за висотою, так і за напрямком в порівнянні з класичним LQR налаштуванням.* ***Методика****. Новий підхід інтегрує SOA з теорією управління LQR. SOA визначає найкращі значення матриць Q і R шляхом мінімізації функції вартості, яка визначається метриками продуктивності системи. Оптимізований за допомогою SOA LQR оцінюється за допомогою моделювання та порівнюється з класичним LQR за ідентичних умов. Кількість становить 50 агентів з максимумом 100 ітерацій для досягнення збіжності.* ***Результати****. Результати моделювання показують, що оптимізований SOA LQR забезпечує значне покращення часу відгуку системи. У порівнянні з класичним LQR, ці результати забезпечують більш короткий час встановлення з 7,35 с до 5,34 с (≈28 %), зменшують перерегулювання (≈3 % порівняно з 30 % у розімкнутому контурі), збільшують демпфування і зменшують коливання. Реакції кутів за висотою та напрямком для кількох схем управління наочно демонструють високу продуктивність запропонованого методу оптимізації.* ***Наукова новизна****. У цій роботі вперше демонструється використання SOA для оптимального налаштування LQR у TRMS. Це відкриває нові можливості для підвищення продуктивності нелінійних систем високого порядку, вказуючи шлях до більш точних та стабільних методів управління в промисловій та аерокосмічній техніці.* ***Практична значимість****. Метод забезпечує ефективне підвищення функціональності складних нелінійних систем без необхідності ручного налаштування та має потенційні галузі застосування у промисловій та аерокосмічній техніці.* Бібл. 38, табл. 3, рис. 4.

Ключові слова: **алгоритм оптимізації «чайка», лінійний квадратичний регулятор, двороторна багатовхідна багатовихідна система, налаштування параметрів, характеристики керування.**

Introduction. The twin rotor multi-input multi-output (MIMO) system (TRMS) remains one of the most highly regarded benchmark platforms within the fields of control research and educational applications, as it effectively represents the challenges of real-world multivariable systems. Constructed to mirror the dynamic properties of a helicopter with two distinct rotors, the TRMS demonstrates notable inter-axis coupling, nonlinear behavior, and open-loop instability, making its control particularly challenging [1–3]. These features make the TRMS an ideal platform for designing and refining advanced control strategies, such as those applied to MIMO systems, where the complex interaction between control variables is critically important [3–5].

Traditionally, robust control methodologies have been employed to address the significant nonlinear cross-coupling inherent in the TRMS. Among these methodologies, the linear quadratic regulator (LQR) is particularly appealing due to its capacity to stabilize the system by minimizing a quadratic performance index that penalizes deviations in state variables and control efforts. Recent studies on TRMS control have confirmed the effectiveness of LQR-based strategies. Adaptive LQR approaches have exhibited superior performance relative to classical LQR and PID controllers, whereas SimMechanics-based LQR designs incorporating steady-state compensation and optimal state-feedback formulations have yielded favorable outcomes for pitch and yaw regulation [6–12].

Traditional PID control is characterized by its simplicity and robustness, rendering it appropriate for systems exhibiting relatively low levels of complexity [13, 14]. However, in the case of nonlinear and tightly coupled MIMO systems like the TRMS, intelligent methodologies are more advantageous. Neural networks [5] and fuzzy logic controllers [15, 16] are capable of addressing uncertainties and complex dynamics without the need for precise models.

Although numerous conventional control methodologies have been employed in the context of TRMS, they frequently do not adequately address its nonlinear dynamics and pronounced pitch–yaw coupling [3, 5, 17]. To enhance regulatory capabilities and robustness, contemporary research endeavors have concentrated on intelligent control methodologies. For example, a butterfly-inspired particle swarm optimization algorithm has been implemented to optimize the parameters of controllers within TRMS [18, 19], while a multi-objective genetic algorithm has contributed to the improvement of stability and tuning precision [20]. Moreover, the integration of inverse modeling with AI-driven controllers has been suggested to effectively manage intricate dynamic interactions [21]. These approaches have succeeded in advancing tracking and damping performance; however, they often fall short in the direct optimization of transient characteristics. To the best of our knowledge, this is among the first studies applying seagull optimization algorithm (SOA) to dynamically tune LQR weighting matrices for TRMS, specifically targeting multi-objective transient improvements.

To address this limitation, the current study introduces a seagull-optimized LQR controller, which is designed to enhance settling time, overshoot, and the overall stability of the system within cross-coupled nonlinear environments.

The **goal** of this study is to optimize the linear quadratic regulator (LQR) weighting matrices Q and R for the TRMS using the seagull optimization algorithm (SOA) to improve transient performance, minimize overshoot, and accelerate stabilization in both pitch and yaw compared to classical LQR tuning.

This paper applies the seagull optimization algorithm to automatically adjust the Q and R matrices of the LQR for the TRMS, with the goal of enhancing the balance between response speed and system stability. In contrast to traditional LQR or PID designs, which often necessitate significant manual tuning due to nonlinearities and intense cross-couplings, the SOA offers a self-optimizing feature that decreases the amount of tuning required. By adaptively probing the Q-R space, the proposed technique results in superior transient performance, including faster rise time, reduced overshoot, and quicker settling when compared to both classical manual tuning methods and less adaptive optimization strategies.

The TRMS model. The TRMS is a laboratory platform that is widely used for teaching and research in multivariable control (Fig. 1). The mechanical design features a beam attached to a pivot that rotates about two orthogonal axes, allowing for coupled pitch and yaw movements similar to the interaction between the main and tail rotors of helicopters [3, 22]. Two DC motor-driven rotors supply the actuation: the «main» rotor primarily influences vertical (pitch) dynamics, whereas the «tail» rotor generates lateral torque for yaw control; the interaction between these channels results in significant cross-coupling, rendering the system a valuable benchmark for study [22–28]. An arm connected to the beam provides stability by balancing angular momentum. The TRMS contains multiple sensors, including incremental encoders and tachogenerators, that monitor 4 essential state variables: pitch angle, yaw angle, pitch angular velocity and yaw angular velocity [28]. Aerodynamic forces and torques are produced by adjusting the rotor speeds, which are controlled via the supply voltage to the DC motors. The system operates in three control modes [3]:

- single degree of freedom (rotors controlled independently);
- two degrees of freedom (both rotors simultaneously);
- decoupled control (cross-couplings modeled and compensated).

In every control mode, the aim is to direct the beam along a defined path, reducing transient errors in the resulting angles. The TRMS system, developed by feedback instruments limited, is an example of a high-level nonlinear system and provides a valuable platform for control studies.

Fig. 1. The general view of the TRMS [23]

Figure 2 presents a simplified diagram of the TRMS. To control TRMS two inputs are used: u_1 (applied to the main rotor) and u_2 (applied to the tail rotor). Dynamic couplings between two motors are the most important feature of the TRMS system. The position beams are measured by incremental encoders, which deliver a relative position signal [28] Therefore, whenever real-time TRMS simulation is executed, it should not be forgotten that setting the proper initial conditions is a critical issue.

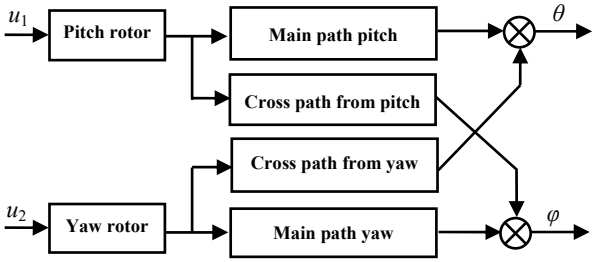

Fig. 2. Diagram of TRMS functions

Modeling and analysis. The modeling requires four linear models: two describing the main dynamic paths from u_1 to φ (pitch) and from u_2 to θ (yaw) and two additional models for the cross-coupling dynamics, from u_1 to θ and from u_2 to φ.

The main rotor (pitch angle) equation is defined by:

$$I_1\ddot{\varphi} = M_1 - M_{FF} - M_{B\varphi} - M_g, \qquad (1)$$

where I_1 is the moment of inertia of vertical plane; M_1 is the gross momentum of the main rotor; M_{FF} is the gravitational momentum; $M_{B\varphi}$ is the momentum due to frictional force; M_g is the gyroscopic momentum.

The momentum is defined as follows:

$$M_1 = a_1\tau_1^2 + b_1\tau_1; \qquad (2) \qquad M_{FF} = M_g \sin\varphi; \quad (3)$$

$$M_{B\varphi} = B_{1\varphi}\dot{\varphi} + B_{2\varphi}\sin(2\varphi)\dot{\varphi}^2; (4) \quad M_g = K_{gy}M_1\dot{\theta}\cos\varphi, (5)$$

where a_1, b_1 are the static characteristic of parameter; $B_{\varphi 1}$, $B_{\varphi 2}$ are the friction momentum function.

The torque τ_1 generated by the main rotor is linked to the input voltage u_1 and is can be represented by the following transfer function:

$$\tau_1 = \frac{K_1}{T_{11}s + T_{10}}u_1, \qquad (6)$$

where K_1 is the gain of the main rotor; T_{11}, T_{10} are the main rotor time constants.

In the same way, we develop the equations of the tail rotor (yaw angle), with the moment produced by the latter described by:

$$I_2\ddot{\theta} = M_2 - M_{B\theta} - M_R, \quad (7)$$

where I_2 is the horizontal rotor moment of inertia; M_2 is the tail rotor's gross momentum; $M_{B\theta}$ is the friction momentum; M_R is the cross-reaction momentum:

$$M_2 = a_2\tau_2^2 + b_2\tau_2; \quad (8)$$

$$M_{B\theta} = B_{1\theta}\dot{\varphi} + B_{2\theta}\text{sign}\dot{\theta}; \quad (9)$$

$$M_R = \frac{K_c(T_0 s + 1)}{T_p s + 1} M_1, \quad (10)$$

where a_2, b_2 are the static characteristic of parameters; K_c is the cross-reaction momentum gain; T_p is the cross-reaction parameter; T_0 is the cross-reaction momentum of the parameter.

The dynamic behavior of «Motor 2» is modeled in a manner analogous to that of «Motor 1» with the torque τ_2 produced by the tail rotor being related to the input voltage u_2 and represented by the following transfer function:

$$\tau_2 = \frac{K_2}{T_{21}s + T_{20}} u_2, \quad (11)$$

where T_{20}, T_{21} are the tail rotor time constants; K_2 is the tail rotor gain.

The main physical parameters of TRMS described in Table 1 play a paramount role concerning the determination of the system dynamic behavior. Besides, these parameters are very important and useful in the development of different control strategies for achieving the wanted performance of the system.

Table 1

TRMS parameters [27]

Parameters and description	Value
I_1 – moment of inertia of vertical plane (pitch axis)	0.068 kg·m^2
I_2 – moment of inertia of horizontal plane (yaw axis)	0.02 kg·m^2
a_1 – static characteristic of parameter	0.00135
b_1 – static characteristic of parameter	0.0924
a_2 – static characteristic of parameter	0.02
b_2 – static characteristic of parameter	0.09
M_g – gravity momentum	0.32 N·m
$B_{\theta 1}$ – parameter of friction momentum	0.006 N·m·s/rad
$B_{\theta 2}$ – parameter of friction momentum	0.001 N·m·s^2/rad
$B_{\varphi 1}$ – parameter of friction momentum	0.1 N·m·s/rad
$B_{\varphi 2}$ – parameter of friction momentum	0.01 N·m·s^2/rad
K_{gv} – parameter of gyroscopic moment	0.05 s/rad
K_1 – motor 1 (pitch) gain	1.1
K_2 – motor 2 (tail) gain	0.8
T_{11} – motor 1 denominator parameter	1.1
T_{10} – motor 1 denominator parameter	1
T_{21} – motor 2 denominator parameter	1
T_{20} – motor 2 denominator parameter	1
T_p – cross-reaction momentum parameter	2
T_0 – cross reaction momentum parameter	3.5
K_c – cross-reaction momentum gain	−0.2

State space representation. The state-space representation of the TRMS describes the system behavior as a set of matrices (***A***, ***B***, ***C***, ***D***), defining how the system state varies with time in response to control inputs:

$$\begin{cases} \dot{\boldsymbol{x}}(t) = \boldsymbol{A}\cdot\boldsymbol{x}(t) + \boldsymbol{B}\cdot\boldsymbol{u}(t); \\ \boldsymbol{y}(t) = \boldsymbol{C}\cdot\boldsymbol{x}(t) + \boldsymbol{D}\cdot\boldsymbol{u}(t), \end{cases} \quad (12)$$

where $\boldsymbol{x}(t)$ is the state vector; $\boldsymbol{u}(t)$ is the control input. The matrices ***A***, ***B***, ***C***, ***D*** define the dynamics of the system. The state variables include the pitch and yaw angles together with their corresponding angular velocities. The control vector $\boldsymbol{u}(t)$ consists of the voltages applied to the main rotor (affecting pitch) and the tail rotor (affecting yaw). The output vector $\boldsymbol{y}(t)$ corresponds to the measured pitch and yaw angles [12].

The system is linearized around the equilibrium points where φ=0 and θ=0, so the nonlinear components become simpler and thus the system simpler to analyze. The state vector $\boldsymbol{x}(t)$ and control input $\boldsymbol{u}(t)$ for the TRMS are delivered by:

$$\boldsymbol{x} = \begin{bmatrix} \varphi \\ \theta \\ \tau_1 \\ \tau_2 \\ M_R \\ \dot{\varphi} \\ \dot{\theta} \end{bmatrix}; \quad (13) \qquad \boldsymbol{u} = \begin{bmatrix} u_1 \\ u_2 \end{bmatrix}. \quad (14)$$

From (5), we can describe our system as

$$\boldsymbol{A} = \begin{bmatrix} 0 & 0 & 0 & 0 & 0 & 1 & 0 \\ 0 & 0 & 0 & 0 & 0 & 0 & 1 \\ 0 & 0 & -0{,}909 & 0 & 0 & 0 & 0 \\ 0 & 0 & 0 & -1 & 0 & 0 & 0 \\ 0 & 0 & 0{,}218181 & 0 & -0{,}5 & 0 & 0 \\ -4{,}70588 & 0 & 1{,}358823 & 0 & 0 & -0{,}088235 & 0 \\ 0 & 0 & 0 & 4{,}5 & -50 & -5 & 0 \end{bmatrix};$$

$$\boldsymbol{B} = \begin{bmatrix} 0 & 0 \\ 0 & 0 \\ 1 & 0 \\ 0 & 0{,}8 \\ -0{,}35 & 0 \\ 0 & 0 \\ 0 & 0 \end{bmatrix}; \quad \boldsymbol{C} = \begin{bmatrix} 1 & 0 & 0 & 0 & 0 & 0 & 0 \\ 0 & 1 & 0 & 0 & 0 & 0 & 0 \end{bmatrix}; \quad \boldsymbol{D} = \begin{bmatrix} 0 & 0 \\ 0 & 0 \end{bmatrix}.$$

LQR formulation. LQR is designed to optimize a quadratic cost function, effectively balancing state regulation with control effort. This makes it particularly well-suited for intricate systems like the TRMS [9, 29]. For the TRMS, the severe cross-coupling and nonlinear dynamics require an energy efficient control approach. In the LQR problem, the cost function is usually given by:

$$J = \int_0^\infty (x^T Q x + u^T R u)\text{d}t, \quad (15)$$

where ***x*** is the state vector, encompassing the pitch and yaw angles as well as their corresponding angular velocities; the vector ***u*** indicates the control inputs that are applied to the rotors; ***Q*** is the state-weighting matrix that is positive semi-definite which penalizes variations in the pitch and yaw states, in contrast ***R*** is the positive definite weighting matrix that prioritizes the reduction of control effort [11, 25, 26].

The purpose of the LQR controller is to determine an optimal state feedback gain matrix ***K***, such that the control law:

$$u(t) = -\boldsymbol{K} \cdot x(t)\,. \quad (16)$$

The matrix $\boldsymbol{K}$ results from solving the algebraic Riccati equation, which balances state regulation (minimizing deviations) and control effort (minimizing energy use). The resulting $\boldsymbol{K}$ provides optimal feedback gains that stabilize the system with high efficiency [25, 29–31].

This work applies SOA to tune the $\boldsymbol{Q}$ and $\boldsymbol{R}$ matrices of the LQR, improving stability and energy efficiency in the nonlinear TRMS. The new method assures improved control performance.

Seagull optimization algorithm (SOA) is a population-based metaheuristic proposed by Dhiman and Kumar in 2019 and is inspired by the migratory and predatory behaviors of seagulls [32]. Migration here refers to periodic motion of gulls while searching for rich food sources to keep their energy levels. During migration, all seagulls avoid any collision with others while updating positions in accordance with information about the best-performing individual in the population [32, 33]. This behavior motivates the seagulls to attack a target in a spiral path through the air. In SOA, migration performs global exploration, and attack performs local exploitation [33]. By integrating both behaviors, the SOA continuously updates the positions of the seagulls to identify the optimal solution. The SOA algorithm is comprised of two main phases: the migration (exploration) phase and the attack (exploitation) phase [33].

Migration phase. The migration behavior of the seagulls involves 3 steps:

1. Collision avoidance.
2. Moving towards the best agent.
3. Convergence towards best agent.

Collision avoidance. To prevent the collision with the neighboring seagulls, a variable A is used to update the position of every seagull:

$$C_s = A \cdot P_s(t), \quad (17)$$

where C_S is the position where the seagull will not collide with another one; $P_s(t)$ is the current position of seagull; t is the iterations number; A is utilized to find the new position of seagulls.

It is updated as [32, 34].

$$A = f_c - t \cdot \left(f_c / T_{\max}\right), \quad (18)$$

where $T_{\max}$ is the maximum number of iterations; f_c (set to 2) is the frequency to control the variable A which is linearly decreases from f_c to 0.

Movement towards the best seagull. After avoiding collisions, the seagulls move toward the best seagull [34–38]. This behavior can be mathematically modeled as follows:

$$M_s = B - (P_{best}(t) - P_s(t)) \quad (19)$$

$$B = 2 \cdot A^2 \cdot rd, \quad (20)$$

where M_s is the direction leading to the optimal location; $P_{best}(t)$ refers to the current position of the most effective search agent; B is the movement behavior of the search agent, which is essential for balancing exploitation and exploration; rd is the randomly generated value that falls between 0 and 1 [36].

Convergence towards best agent. After determining the convergence direction, the seagull move toward the best search agent [33, 38]:

$$D_s = \left| C_s + M_s \right|, \quad (21)$$

where D_S is the distance between seagulls and the best search agent.

Attacking phase. In the second phase, after reaching a new location, seagulls execute a spiral attack on prey. This predatory behavior can be mathematically modeled as follows:

$$P(t) = D_s\, x \cdot y \cdot z + P_{best}(t), \quad (22)$$

where $P(t)$ retains the best solution; x, y, z are the spiral components:

$$x = r \cdot \cos\theta\,; \quad (23) \qquad y = r \cdot \sin\theta\,; \quad (24)$$

$$z = r \cdot \theta\,; \quad (25) \qquad r = \mu \cdot e^{\theta v}, \quad (26)$$

where r is the spiral radius during the seagull's motion, while μ and v are the correlation constants that define the spiral shape; θ is the angle, which is a random value within the range of $[0, 2\pi]$ [35].

In the standard SOA, both μ and v are set to 1. The updated position of the seagull is determined using equations (23)–(26), as illustrated:

$$P_s(t+1) = D_s\, x \cdot y \cdot z + P_{best}(t), \quad (27)$$

where $P_s(t+1)$ is the new position of the search agent.

Results and discussions. In this study, SOA was utilized for the TRMS. The population size was set to 50 agents, which is a balance between exploration capability and computational cost. The optimization process was allowed to perform at a maximum of 100 iterations $T_{\max}$=100, therefore providing sufficient time for convergence.

The frequency control parameter f_c was set as 2, and the movement behavior parameter A started at 2 and linearly decreased to 0 over iterations to reduce collisions and enhance convergence. The best position $P_{best}(t)$ was updated incrementally, improving the global best solution at each iteration A random variable rd uniformly generated in the range of 0 to 1 was included to maintain a balance between exploration and exploitation by introducing stochastic variability. In addition, collision avoiding mechanisms and distance calculation based on the current position of the agents and their iteration steps were implemented to ensure an optimally balanced and effective search process. As shown in Table 2, in open loop the system is rapid (rise time 0.896 s), but unstable with lengthy overshoot of 30.34 % and settling time of 65.88 s, indicating an under damped system.

Table 2

Temporal characteristics for pitch response

Characteristic of pitch	Open loop	Classical LQR	SOA-optimized LQR
Rise time, s	0.896	4.0069	1.2379
Settling time, s	65.88	7.3462	5.3055
Overshoot, %	30.34	1.3589	3.0618

With the classical LQR controller, the TRMS becomes stable with a slower rise time of 4.0069 s, settling time of 7.3462 s and smaller overshoot of 1.3589 %, showing improved damping. The performance of SOA-optimized is accomplished with the rise time of 1.2379 s, settling time of 5.3055 s and controlled overshoot of 3.0618 %, achieving a balance between speed and stability.

The TRMS in open-loop yaw (Table 3) response is very slow with a rise time of 316.18 s and a settling time of 455.89 s, indicating severe instability. The classical LQR controller enhances the performance significantly, by minimizing the rise time to 0.75 s and settling time to 6.28 s, and an overshoot of 10.72 %, which shows a minor oscillatory response. The SOA-optimized LQR further reduces these values, the rise time coming to 0.48 s and settling time coming to 2.67 s, which shows accelerated convergence. The overshoot is reduced to 9.71 %, indicating a damped response.

Table 3

Temporal characteristics for yaw response

Characteristic of yaw	Open loop	Classical LQR	SOA-optimized LQR
Rise time, s	316.18	0.75	0.48
Settling time, s	455.89	6.28	2.67
Overshoot, %	0	10.72	9.71

For pitch response, the SOA-optimized LQR decreases settling time to 5.3055 s (7.3462 s for classical LQR) with a 28 % decrease but keeps the overshoot in control at 3.0618 %. For yaw response also, the settling time decreases from 6.28 s to 2.67 s, a significant 57 % decrease, with an eased overshoot of 9.71 %.

Figures 3, 4 illustrate the pitch and yaw angle response of the system under 3 control modes: open-loop, classical LQR, and SOA-optimized LQR.

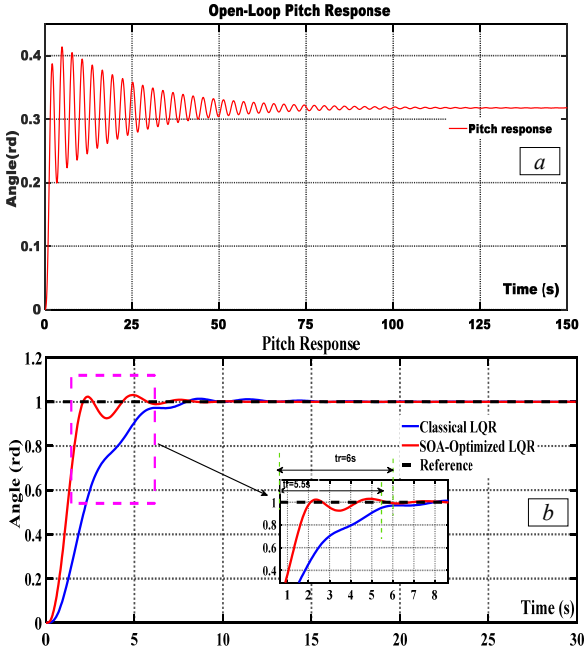

Fig. 3. Temporal characteristics of pitch responses under open loop (*a*); with LQR and SOA controller (*b*)

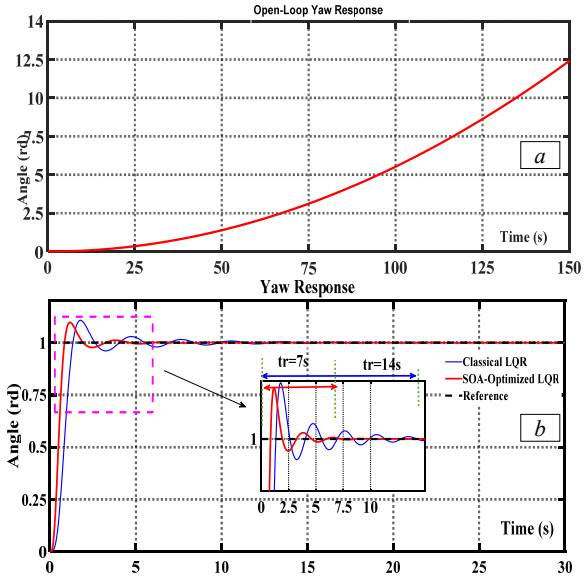

Fig. 4. Temporal characteristics of yaw responses under open loop (*a*); with LQR and SOA controller (*b*)

The SOA-optimized LQR shows significant improvement in settling time and stability compared to open-loop and standard LQR control. Although the rise time is slightly increased, the settling time and overshoot have been significantly reduced, realizing a balance speed between stability. These results validate the performance of SOA in regulating control parameters of deeply coupled complex MIMO systems as well as in dealing with nonlinearities.

Conclusions. Twin rotor MIMO system was effectively controlled with an SOA-optimized LQR algorithm, demonstrating improved dynamic response (pitch settling ≈28 % faster; yaw ≈57 % faster vs classical LQR) and enhanced stability compared to open-loop (overshoot ≈3 % vs 30 % open-loop pitch) and standard LQR control strategies.

This research proposed a new contribution by combining the seagull optimization algorithm with systematic parameter space exploration, adding a new reference for adaptive control of dynamic systems. The limited trade-offs observed in this study indicate potential for future progress.

Future research might focus on real-time implementation, addressing computational complexity and robustness against external disturbances, in order to enable reliable experimental applications.

Conflict of interest. The authors of the article declare that there is no conflict of interest.

REFERENCES

1. Milovanovic M.B., Antic D.S., Milojkovic M.T., Spasic M.D. Adaptive Control of Nonlinear MIMO System With Orthogonal Endocrine Intelligent Controller. *IEEE Transactions on Cybernetics*, 2022, vol. 52, no. 2, pp. 1221-1232. doi: https://doi.org/10.1109/TCYB.2020.2998505.

2. Cao C., Huang X., Cao W., Wang H., Yang Y., Xu J. MIMO Control of a Twin Rotor Aerodynamical System (TRAS). *2025 9th International Conference on Robotics, Control and Automation (ICRCA)*, 2025, pp. 265-269. doi: https://doi.org/10.1109/ICRCA64997.2025.11011049.

3. Ebirim K.U., Horri N.M., Prempain E. A 2DoF Twin Rotor MIMO System for Teaching and Research. *IFAC-PapersOnLine*, 2024, vol. 58, no. 16, pp. 6-11. doi: https://doi.org/10.1016/j.ifacol.2024.08.453.

4. Danh H.D., Van C.N., Van Q.V. Tracking Iterative Learning Control of TRMS using Feedback Linearization Model with Input Disturbance. *Journal of Robotics and Control (JRC)*, 2025, vol. 6, no. 1, pp. 446-455. doi: https://doi.org/10.18196/jrc.v6i1.25579.

5. Han S.-Y., Zhang C.-Y. ASMAC: An Adaptive Slot Access MAC Protocol in Distributed VANET. *Electronics*, 2022, vol. 11, no. 7, art. no. 1145. doi: https://doi.org/10.3390/electronics11071145.

6. Dutta L., Das D.K. Nonlinear Disturbance Observer Based Adaptive Explicit Nonlinear Model Predictive Control Design for a Class of Nonlinear MIMO System. *IEEE Transactions on Aerospace and Electronic Systems*, 2022, vol. 59, no. 2, pp. 1965-1979. doi: https://doi.org/10.1109/TAES.2022.3211252.

7. Shah A.Q., Awais M., Zafar M., Ahmed A., Mudassar M., Muneer M., Saif M., Razzaq A., Jang S.-H., Kim S., Park Y. A comparative study of linear control strategies on the aerodynamics twin rotor system. *Journal of Mechanical Science and Technology*, 2023, vol. 37, no. 8, pp. 4301-4310. doi: https://doi.org/10.1007/s12206-023-0746-5.

8. Bilal H., Yin B., Aslam M.S., Anjum Z., Rohra A., Wang Y. A practical study of active disturbance rejection control for rotary flexible joint robot manipulator. *Soft Computing*, 2023, vol. 27, no. 8, pp. 4987-5001. doi: https://doi.org/10.1007/s00500-023-08026-x.

9. Faisal R.F., Abdulwahhab O.W. Design of an Adaptive Linear Quadratic Regulator for a Twin Rotor Aerodynamic System. *Journal of Control, Automation and Electrical Systems*, 2021, vol. 32, no. 2, pp. 404-415. doi: https://doi.org/10.1007/s40313-020-00682-w.

10. Fahmizal, Nugroho H.A., Cahyadi A.I., Ardiyanto I. Twin Rotor MIMO System Control using Linear Quadratic Regulator with Simechanics. *2021 7th International Conference on Electrical, Electronics and Information Engineering (ICEEIE)*, 2021, pp. 301-306. doi: https://doi.org/10.1109/ICEEIE52663.2021.9616893.

11. Ranjan K.V., Laxmi V. Design of an Optimal Controller for a Twin Rotor Mimo System (TRMS). *2022 International Conference on*

Sustainable Computing and Data Communication Systems (ICSCDS), 2022, pp. 950-959. doi: https://doi.org/10.1109/ICSCDS53736.2022.9760778.
12. Darsouni Z., Rezgui S.E., Benalla H., Rebahi F., Boumendjel M.A.M. Ensuring service continuity in electric vehicles with vector control and linear quadratic regulator for dual star induction motors. *Electrical Engineering & Electromechanics*, 2025, no. 2, pp. 24-30. doi: https://doi.org/10.20998/2074-272X.2025.2.04.
13. Latreche K., Taleb R., Bentaallah A., Toubal Maamar A.E., Helaimi M., Chabni F. Design and experimental implementation of voltage control scheme using the coefficient diagram method based PID controller for two-level boost converter with photovoltaic system. *Electrical Engineering & Electromechanics*, 2024, no. 1, pp. 3-9. doi: https://doi.org/10.20998/2074-272X.2024.1.01.
14. Alnaib I.I., Alsammak A.N. Optimization of fractional PI controller parameters for enhanced induction motor speed control via indirect field-oriented control. *Electrical Engineering & Electromechanics*, 2025, no. 1, pp. 3-7. doi: https://doi.org/10.20998/2074-272X.2025.1.01.
15. Boudia A., Messalti S., Zeghlache S., Harrag A. Type-2 fuzzy logic controller-based maximum power point tracking for photovoltaic system. *Electrical Engineering & Electromechanics*, 2025, no. 1, pp. 16-22. doi: https://doi.org/10.20998/2074-272X.2025.1.03.
16. Khemis A., Boutabba T., Drid S. Model reference adaptive system speed estimator based on type-1 and type-2 fuzzy logic sensorless control of electrical vehicle with electrical differential. *Electrical Engineering & Electromechanics*, 2023, no. 4, pp. 19-25. doi: https://doi.org/10.20998/2074-272X.2023.4.03.
17. Kadri K., Boudjema F., Bouzid Y., Ouahab B., Draris H.I. A linear Active Disturbance Rejection Control based PSO to control Twin Rotor MIMO System with experimental validation. *2023 International Conference on Electrical Engineering and Advanced Technology (ICEEAT)*, 2023, pp. 1-7. doi: https://doi.org/10.1109/ICEEAT60471.2023.10425852.
18. Sivadasan J., Shiney J.R.J. Modified nondominated sorting genetic algorithm-based multiobjective optimization of a cross-coupled nonlinear PID controller for a Twin Rotor System. *Journal of Engineering and Applied Science*, 2023, vol. 70, no. 1, art. no. 133. doi: https://doi.org/10.1186/s44147-023-00305-6.
19. Cabuker A.C., Almali M.N., Parlar I. Evaluation of controller parameters on the twin rotor multiple input multiple output system using butterfly-based particle swarm optimization. *Journal of Scientific Reports-A*, 2023, no. 052, pp. 174-189. doi: https://doi.org/10.59313/jsr-a.1198441.
20. Çelebi B., Bilgiç B. Optimizing TRMS stability: a multi-objective genetic algorithm approach to PID controller design. *Engineering Computations*, 2025, vol. 42, no. 2, pp. 710-721. doi: https://doi.org/10.1108/EC-06-2024-0476.
21. Al-Talabi A., Fahad T.O., Mohammed A.A., Mary A.H. Inverse modeling, analysis and control of twin rotor aerodynamic systems with optimized artificial intelligent controllers. *PLOS One*, 2025, vol. 20, no. 5, art. no. e0322999. doi: https://doi.org/10.1371/journal.pone.0322999.
22. Gopmandal F., Ghosh A. LQR-based MIMO PID control of a 2-DOF helicopter system with uncertain cross-coupled gain. *IFAC-PapersOnLine*, 2022, vol. 55, no. 22, pp. 183-188. doi: https://doi.org/10.1016/j.ifacol.2023.03.031.
23. Aidoud M., Feliu-Batlle V., Sebbagh A., Sedraoui M. Small signal model designing and robust decentralized tilt integral derivative TID controller synthesizing for twin rotor MIMO system. *International Journal of Dynamics and Control*, 2022, vol. 10, no. 5, pp. 1657-1673. doi: https://doi.org/10.1007/s40435-022-00916-6.
24. Sajjad Moosapour S., Mehdipour H., Keramatzadeh M. Sliding Mode Disturbance Observer-Based Control of a Laboratory Twin Rotor Multi Input-Multi Output System. *IEEE Access*, 2025, vol. 13, pp. 394-406. doi: https://doi.org/10.1109/ACCESS.2024.3523850.
25. Tran A.-M.D., Vu T.V. Robust MIMO LQR Control with Integral Action for Differential Drive Robots: A Lyapunov-Cost Function Approach. *Engineering, Technology & Applied Science Research*, 2025, vol. 15, no. 4, pp. 24775-24781. doi: https://doi.org/10.48084/etasr.11583.
26. Dehnavi V.S., Shafiee M. LQR for Generalized Systems Using Metaheuristic Algorithms Based on Disturbance Observer. *2020 28th Iranian Conference on Electrical Engineering (ICEE)*, 2020, pp. 1-5. doi: https://doi.org/10.1109/ICEE50131.2020.9260723.
27. Zeghlache S., Benyettou L., Djerioui A., Ghellab M.Z. Twin Rotor MIMO System Experimental Validation of Robust Adaptive Fuzzy Control Against Wind Effects. *IEEE Systems Journal*, 2022, vol. 16, no. 1, pp. 409-419. doi: https://doi.org/10.1109/JSYST.2020.3034993.
28. Ezekiel D.M., Samikannu R., Matsebe O. Pitch and Yaw Angular Motions (Rotations) Control of the 1-DOF and 2-DOF TRMS: A Survey. *Archives of Computational Methods in Engineering*, 2021, vol. 28, no. 3, pp. 1449-1458. doi: https://doi.org/10.1007/s11831-020-09423-3.
29. Senoussaoui A., Chenafa M., Sahraoui A., Kacimi A., Houcine R. LQGi/LTR controller with integrators and feedforward controller applied to a Twin Rotor MIMO System. *Przeglad Elektrotechniczny*, 2021, vol. 97, no. 4, pp. 48-53. doi: https://doi.org/10.15199/48.2021.04.08.
30. Faisal R.F., Abdulwahhab O.W. Design of an Adaptive Linear Quadratic Regulator for a Twin Rotor Aerodynamic System. *Journal of Control, Automation and Electrical Systems*, 2021, vol. 32, no. 2, pp. 404-415. doi: https://doi.org/10.1007/s40313-020-00682-w.
31. Nekrouf S., Chekroun S. Optimal controller design for a birotor helicopter. *Przegląd Elektrotechniczny*, 2021, vol. 97, no. 11, pp. 93-96. doi: https://doi.org/10.15199/48.2021.11.16.
32. Kumar V., Kumar D., Kaur M., Singh D., Idris S.A., Alshazly H. A Novel Binary Seagull Optimizer and its Application to Feature Selection Problem. *IEEE Access*, 2021, vol. 9, pp. 103481-103496. doi: https://doi.org/10.1109/ACCESS.2021.3098642.
33. Jiang H., Yang Y., Ping W., Dong Y. A Novel Hybrid Classification Method Based on the Opposition-Based Seagull Optimization Algorithm. *IEEE Access*, 2020, vol. 8, pp. 100778-100790. doi: https://doi.org/10.1109/ACCESS.2020.2997791.
34. Hanif M., Mohammad N., Biswas K., Harun B. Seagull Optimization Algorithm for Solving Economic Load Dispatch Problem. *2023 International Conference on Electrical, Computer and Communication Engineering (ECCE)*, 2023, pp. 1-6. doi: https://doi.org/10.1109/ECCE57851.2023.10101516.
35. Hou P., Liu J., Ni F., Zhang L. Hybrid Strategies Based Seagull Optimization Algorithm for Solving Engineering Design Problems. *International Journal of Computational Intelligence Systems*, 2024, vol. 17, no. 1, art. no. 62. doi: https://doi.org/10.1007/s44196-024-00439-2.
36. Ragab M., Alshehri S., Alhakamy N.A., Alsaggaf W., Alhadrami H.A., Alyami J. Machine Learning with Quantum Seagull Optimization Model for COVID-19 Chest X-Ray Image Classification. *Journal of Healthcare Engineering*, 2022, vol. 2022, art. no. 6074538. doi: https://doi.org/10.1155/2022/6074538.
37. Wang J., Li Y., Hu G. Hybrid seagull optimization algorithm and its engineering application integrating Yin–Yang Pair idea. *Engineering with Computers*, 2022, vol. 38, no. 3, pp. 2821-2857. doi: https://doi.org/10.1007/s00366-021-01508-2.
38. Aribowo W., Muslim S., Achmad F., Hermawan A.C. Improving Neural Network Based on Seagull Optimization Algorithm for Controlling DC Motor. *Jurnal Elektronika Dan Telekomunikasi*, 2021, vol. 21, no. 1, pp. 48-54. doi: https://doi.org/10.14203/jet.v21.48-54.

Received 16.07.2025
Accepted 07.09.2025
Published 02.01.2026

H. Mostefaoui[1], *Doctor of Electrical Engineering,*
S. Tahraoui[1], *Doctor of Electrical Engineering, Associate Professor,*
M. Souaihia[2], *Doctor of Electrical Engineering,*
R. Taleb[2], *Full Professor,*
M. Mostefaoui[2], *Doctor, Associate Professor,*
[1] Electrical Engineering Department, 2SAIL Laboratory,
Hassiba Benbouali University, Algeria,
e-mail: h.mostefaoui@univ-chlef.dz (Corresponding Author);
s.tahraoui@univ-chlef.dz
[2] Electrical Engineering Department,
Laboratoire Génie Electrique et Energies Renouvelables (LGEER),
Hassiba Benbouali University, Algeria,
e-mail: m.souaihia@univ-chlef.dz; r.taleb@univ-chlef.dz;
m.mostefaoui@univ-chlef.dz

How to cite this article:
Mostefaoui H., Tahraoui S., Souaihia M., Taleb R., Mostefaoui M. Advanced control of twin rotor multi-input multi-output systems using seagull optimization for linear quadratic regulator tuning. *Electrical Engineering & Electromechanics*, 2026, no. 1, pp. 38-43. doi: https://doi.org/10.20998/2074-272X.2026.1.05